JAMA Ophthalmology | Original Investigation

Detecting Glaucoma With a Portable Brain-Computer Interface for Objective Assessment of Visual Function Loss

Masaki Nakanishi, PhD; Yu-Te Wang, PhD; Tzyy-Ping Jung, PhD; John K. Zao, PhD; Yu-Yi Chien, PhD; Alberto Diniz-Filho, MD; Fabio B. Daga, MD; Yuan-Pin Lin, PhD; Yijun Wang, PhD; Felipe A. Medeiros, MD, PhD

IMPORTANCE The current assessment of visual field loss in diseases such as glaucoma is affected by the subjectivity of patient responses and the lack of portability of standard perimeters.

OBJECTIVE To describe the development and initial validation of a portable brain-computer interface (BCI) for objectively assessing visual function loss.

DESIGN, SETTING, AND PARTICIPANTS This case-control study involved 62 eyes of 33 patients with glaucoma and 30 eyes of 17 healthy participants. Glaucoma was diagnosed based on a masked grading of optic disc stereophotographs. All participants underwent testing with a BCI device and standard automated perimetry (SAP) within 3 months. The BCI device integrates wearable, wireless, dry electroencephalogram and electrooculogram systems and a cellphone-based head-mounted display to enable the detection of multifocal steady state visual-evoked potentials associated with visual field stimulation. The performances of global and sectoral multifocal steady state visual-evoked potentials metrics to discriminate glaucomatous from healthy eyes were compared with global and sectoral SAP parameters. The repeatability of the BCI device measurements was assessed by collecting results of repeated testing in 20 eyes of 10 participants with glaucoma for 3 sessions of measurements separated by weekly intervals.

MAIN OUTCOMES AND MEASURES Receiver operating characteristic curves summarizing diagnostic accuracy. Intraclass correlation coefficients and coefficients of variation for assessing repeatability.

RESULTS Among the 33 participants with glaucoma, 19 (58%) were white, 12 (36%) were black, and 2 (6%) were Asian, while among the 17 participants with healthy eyes, 9 (53%) were white, 8 (47%) were black, and none were Asian. The receiver operating characteristic curve area for the global BCI multifocal steady state visual-evoked potentials parameter was 0.92 (95% CI, 0.86-0.96), which was larger than for SAP mean deviation (area under the curve, 0.81; 95% CI, 0.72-0.90), SAP mean sensitivity (area under the curve, 0.80; 95% CI, 0.69-0.88; $P = .03$), and SAP pattern standard deviation (area under the curve, 0.77; 95% CI, 0.66-0.87; $P = .01$). No statistically significant differences were seen for the sectoral measurements between the BCI and SAP. Intraclass coefficients for global and sectoral parameters ranged from 0.74 to 0.92, and mean coefficients of variation ranged from 3.03% to 7.45%.

CONCLUSIONS AND RELEVANCE The BCI device may be useful for assessing the electrical brain responses associated with visual field stimulation. The device discriminated eyes with glaucomatous neuropathy from healthy eyes in a clinically based setting. Further studies should investigate the feasibility of the BCI device for home-based testing as well as for detecting visual function loss over time.

JAMA Ophthalmol. 2017;135(6):550-557. doi:10.1001/jamaophthalmol.2017.0738
Published online April 27, 2017.

Supplemental content

Author Affiliations: Visual Performance Laboratory, University of California–San Diego, La Jolla (Nakanishi, Diniz-Filho, Daga, Medeiros); Swartz Center for Computational Neuroscience, University of California–San Diego, La Jolla (Y.-T. Wang, Jung, Chien, Lin, Y. Wang); Department of Computer Science, National Chiao Tung University, Hsinchu, Taiwan (Zao, Chien).

Corresponding Author: Felipe A. Medeiros, MD, PhD, Visual Performance Laboratory, University of California–San Diego, 9500 Gilman Dr, La Jolla, CA 92093-0946 (fmedeiros@ucsd.edu).

Glaucoma is a group of optic neuropathies that have a progressive degeneration of retinal ganglion cells and their axons, resulting in a characteristic appearance of the optic disc and visual field loss. Assessing functional loss in glaucoma has traditionally been done using standard automated perimetry (SAP). However, SAP requires considerable subjective input from the patient and is limited by large test-retest variability.[1] As SAP testing is generally performed in clinically based settings, limited resources frequently result in patients not undergoing the necessary number of tests over time, which may result in patients receiving a late diagnosis or a delayed detection of progression.

The objective assessment of visual field damage has been attempted by using visual-evoked potential (VEP) techniques, especially multifocal VEP (mfVEP). The multifocal technique allows many areas of the retina to be stimulated simultaneously and for responses from each part of the visual field to be obtained. Results published using mfVEP have demonstrated a good correspondence between visual field sensitivity and local mfVEP responses.[2] However, mfVEP recording techniques can only be performed with nonportable devices in clinically or laboratory-based settings, requiring a cumbersome setup for placing electrodes, preparing the skin, and applying gel, which are time-consuming processes that may be uncomfortable for the patient.

Progress has been recently achieved in developing brain-computer interfaces (BCIs) that can process electrical brain signals such as VEPs. Brain-computer interfaces rely on steady state visual-evoked potentials (SSVEPs), which, in contrast to the transient event-related potentials, are elicited by rapid flickering stimulation, producing a brain response characterized by a "quasisinusoidal" waveform that has frequency components that are constant in amplitude and phase.[3] Steady state VEPs have desirable properties for assessing the integrity of the visual system. The technique is faster than mfVEP and less susceptible to artifacts produced by blinking and eye movements[4] as well as electromyographic noise contamination,[5] and it may present a better signal to noise ratio.[3,6-11] The feasibility of acquiring wireless SSVEP data has also been demonstrated for monitoring high temporal resolution brain dynamics without requiring conductive gels to be applied to the scalp.[12-16] Additionally, advanced analytical techniques, such as an independent component analysis, have been successfully used to improve the detectability of SSVEP signals.[17-26] These advances in using SSVEP techniques make it an ideal candidate technique for developing a portable method of objectively assessing visual field loss in glaucoma.

In this study, we present the development and initial validation of the nGoggle (nGoggle Inc), a BCI for objectively assessing visual field deficits using multifocal SSVEPs (mfSSVEPs). The portable platform integrates a wearable, wireless, dry electroencephalogram (EEG) system and a head-mounted display that allow for the monitoring of the electrical brain activity associated with visual field stimulation. We investigated the ability of nGoggle measurements to discriminate glaucomatous from healthy eyes as well as their repeatability.

Key Points

Question Is a portable brain-computer interface used to objectively assess visual function able to discriminate glaucomatous eyes from healthy eyes?

Findings This case-control study used a portable brain-computer interface that assesses multifocal steady state visual-evoked potentials in response to visual field stimulation. The parameters of this device were able to discriminate eyes with glaucomatous optic neuropathy from healthy eyes, as compared with standard automated perimetry.

Meaning The brain-computer interface shows promise as a portable device for objectively assessing visual function loss as it was able to detect glaucomatous damage in a clinically based study.

Methods

This was a prospective study conducted at the Visual Performance Laboratory of the University of California–San Diego. All participants underwent a comprehensive ophthalmologic examination, including medical history, best-corrected visual acuity, a slitlamp biomicroscopy, intraocular pressure measurement with Goldman tonometry, a gonioscopy, a dilated stereoscopic fundus examination, stereoscopic optic disc photography, and SAP. Only participants with open angles on gonioscopy were included. Participants were excluded if they presented with a best-corrected visual acuity of less than 20/40, spherical refraction outside ±5.0 D and/or cylinder correction outside 3.0 D, or any ocular/systemic disease besides glaucoma that could affect the optic nerve or the visual field, such as coexisting retinal disease.

Diagnosing glaucoma was based on the presence of glaucomatous optic neuropathy as determined by the masked grading of optic disc stereophotographs by 2 graders. If these graders disagreed, a third observer served as an adjudicator. Simultaneous stereoscopic optic disc photographs (TRC-SS; Topcon Instrument Corporation of America) were reviewed using a stereoscopic viewer (Asahi Pentax Stereo Viewer II, Asahi Optical Co). Signs of glaucomatous optic neuropathy were considered as rim thinning, excavation, the presence of retinal nerve fiber layer defects, and a cup-disc ratio asymmetry more than 0.2. Healthy participants were recruited from the general population and were required to have a normal optic disc appearance in both eyes as well as no history of elevated intraocular pressure.

The institutional review board and human subjects committee of the University of California–San Diego approved all the methods, which adhered to the tenets of the Declaration of Helsinki for research involving human participants and were conducted in accordance with the regulations of the Health Insurance Portability and Accountability Act. All participants provided written informed consent. The study design and implementation started in April 2015, with data collection performed from October 2015 to July 2016. The study was completed in October 2016.

Figure 1. The nGoggle, a Portable Brain-Computer Interface for Assessment of Visual Function

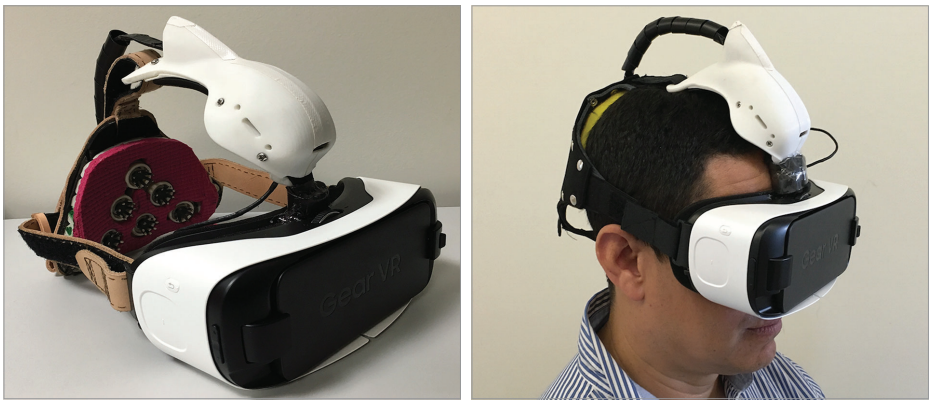

A. The nGoggle consists of a portable multifocal steady state visual-evoked potential–based visual function assessment platform, integrating wearable, wireless, dry electroencephalogram and electrooculogram systems and a head-mounted display,
B. Photograph of a participant undergoing testing with the nGoggle.

The nGoggle

The nGoggle consists of a portable, objective BCI integrating wireless, easy-to-wear dry EEG and electrooculogram (EOG) systems and a head-mounted display (**Figure 1**). The device contains a wireless neuromonitoring system-on-module, equipped with a dual-core embedded processor, assorted input/output interfaces, and a dual-band 602.11a/b/g/n wireless fidelity + Bluetooth 4 radio. The device also detects 3-dimensional linear acceleration and 3-dimensional angular velocity simultaneously at 200 samples per second.

The nGoggle captures electrophysiological signals from 6 EEG and 4 EOG channels. It uses customized flexible polymer-based dry EEG electrodes and foam-based dry EOG electrodes for no-preparation wearing. Integrated low-noise preamplifiers and 24-bit sigma-delta analog-digital converters can perform synchronous data sampling at up to 1000 samples per second. Each channel is equipped with a lead-off detection capability to check whether the electrode makes good contact with the scalp. The mfSSVEP Visual Stimuli Rendering Mobile App is based on the OpenGL ES, version 2.0 (Khronos Group) to render multifrequency multifocal visual stimuli on an Android phone with a 60-frames-per-second display. The Signal Processing and Data Analysis Tool is equipped with a proprietary software that has been used in our high-speed BCI speller[27-29] that holds successive world records and was adapted to estimate the relative amplitudes, signal-to-noise ratios, phases, and correlations of mfSSVEP with multifocal visual stimuli.

The 6 dry EEG sensors on the nGoggle were located at positions Pz, PO4, PO3, O1, Oz, and O2 according to the 10-20 international system. Visual stimuli consisted of 2 patterns of 20 sectors involving the central 35° field of view, flickering at different frequencies (8-11.8 Hz with an interval of 0.2 Hz) (eFigure 1 in the Supplement). The platform uses a frequency approximation approach to approximate flexible frequencies with variable number of frames in a stimulating period. This allows for a successful presentation of several visual stimuli with different frequencies, overcoming limitations from the fixed display frequency rate. We have previously presented details of this technique.[30,31] Two patterns of visual stimuli were presented separately to enhance the signal-to-noise ratio in eliciting SSVEPs. The experiment consisted of 3 A-pattern sessions and 3 B-pattern sessions for each eye. Participants were instructed to sit in a comfortable chair and to gaze at a red dot located in the center of visual stimuli. Each session per eye contained 30 trials of 6-second duration, including 5 seconds of visual stimulation followed by a 1-second short break, totaling 3 minutes. Ninety-second data epochs composed of 6-channel mfSSVEPs were extracted from the recorded EEG data after bandpass filtering from 6 Hz to 25 Hz. Epochs with artifacts caused by fixation losses were detected by analyzing EOG channels and were removed automatically using a customized algorithm. In this study, epochs that had EOG amplitudes that exceeded a predefined threshold of 150 were removed.[22]

Spatial filters based on a canonical correlation analysis (CCA) were applied to data epochs according to a previously described technique.[32,33] The CCA extends the ordinary correlation analysis to measure the underlying correlation between 2 sets of multidimensional variables. In the analysis of SSVEPs, the coefficients obtained by the CCA between EEG signals and synthesized computational models of SSVEPs were used as a spatial filter to remove noisy channels, leading to a measure that was robust to artifacts and spontaneous EEG activities.[33] As CCA represents a correlation measure, it varies from 0 to 1, with higher values indicating a higher correlation between evoked EEG signals and ideal waveforms of SSVEPs. Therefore, healthy eyes would likely show higher CCA values than eyes with glaucomatous neuropathy.

A global metric representing the overall mfSSVEP-CCA metric for each eye was calculated as the average of values for each sector and used in the study. Additionally, we also calculated sectoral measurements to correspond to the superior, inferior, temporal, and central areas of the field of view, approximating a previously published structure-function map by Garway-Heath et al[34] (eFigure 2 in the Supplement).

Standard Automated Perimetry

Standard automated perimetry testing was conducted using program 24-2 and the SITA Standard testing algorithm (Humphrey Visual Field Analyzer II, Carl Zeiss Meditec). Visual fields with more than 25% fixation losses or more than 15% false-positive

Table 1. Demographic and Clinical Variables of the Glaucomatous and Healthy Participants/Eyes Included in the Study

Variable	Glaucoma (n = 62 Eyes of 33 Participants)	Healthy (n = 30 Eyes of 17 Participants)	*P* Value
Age, mean (SD), y	68.2 (11.0)	66.1 (9.9)	.57
Women, No. (%)	8 (47)	16 (48)	.92
Race/ethnicity, No. (%)			
White	19 (58)	9 (53)	.50
Black	12 (36)	8 (47)	
Asian	2 (6)	0	
SAP, median (IQR), dB			
MS	24.8 (17.5-27.7)	29.1 (26.8-30.7)	<.001
MD	−4.0 (−12.7 to −1.8)	−0.6 (−2.4 to 1.0)	<.001
PSD	4.7 (2.2-9.9)	1.9 (1.4-3.0)	<.001
nGoggle global mfSSVEP, mean (SD)	0.289 (0.020)	0.334 (0.024)	<.001

Abbreviations: IQR, interquartile range; MD, mean deviation; mfSSVEP, multifocal steady state visual-evoked potential; MS, mean sensitivity, PSD, pattern standard deviation; SAP, standard automated perimetry.

Table 2. Areas Under the Receiver Operating Characteristic Curves and Sensitivities Fixed Specificities to Discriminate Glaucoma From Healthy Eyes for the nGoggle Global Multifocal Steady State Visual-Evoked Parameter and Standard Automated Perimetry Parameters

Measure	AUC (95% CI)	Sensitivity for Specificity, % (95% CI)	
		80%	90%
nGoggle global mfSSVEP	0.92 (0.86-0.96)	85 (71-95)	71 (53-87)
SAP			
MD	0.81 (0.72-0.90)	64 (45-82)	43 (23-68)
MS	0.80 (0.69-0.88)	60 (39-77)	39 (18-59)
PSD	0.77 (0.66-0.86)	61 (40-75)	47 (24-66)

Abbreviations: AUC, Areas under the receiver operating characteristic; MD, mean deviation; mfSSVEP, multifocal steady state visual evoked potential; MS, mean sensitivity, PSD, pattern standard deviation; SAP, standard automated perimetry.

result errors were excluded. The SAP threshold sensitivities were obtained for each target location and averaged to calculate a global mean sensitivity value. The 2 locations just above and below the blind spot were not included in the analysis. The SAP mean deviation (MD) and pattern standard deviation (PSD) were also evaluated as global parameters. Additionally, threshold sensitivities were averaged to correspond to nGoggle sectors (eFigure 2 in the Supplement). Participants underwent testing with SAP and the nGoggle within 3 months.

Statistical Analyses

Receiver operating characteristic (ROC) curves were constructed to assess the diagnostic ability of the nGoggle and SAP in discriminating glaucomatous eyes from normal eyes. The ROC curve provides the tradeoff between the sensitivity and 1-specificity. The area under the ROC curve (AUC) was used to summarize the diagnostic accuracy of each parameter. An AUC of 1.0 represents perfect discrimination, whereas an area of 0.5 represents chance discrimination.

To account for using both eyes of the same participant in the analyses, a bootstrap resampling procedure (n = 1000 resamples) was used to derive confidence intervals. To account for the correlation between eyes, the cluster of data for the participant was considered as the unit of resampling to adjust standard errors. This procedure has been previously used to adjust for the presence of multiple correlated measurements from the same unit.[35]

Sample Size and Power Calculation

For this investigation of diagnostic accuracy, sample size was calculated to detect a minimally significant difference of 0.1 between the AUCs of diagnostic parameters, with a correlation of 0.6 between measurements and a 2 to 1 ratio of glaucoma to healthy eyes. For a power of 80%, the required sample size was calculated as 54 glaucomatous and 27 healthy eyes.

Repeatability Assessment

An initial assessment of the repeatability of the nGoggle measurements was obtained by collecting repeated testing among 20 eyes of 10 participants with glaucoma. Participants had 3 sessions of measurements separated by weekly intervals between sessions. For each eye, a coefficient of variation was calculated as the ratio of the SD of the 3 measurements and the corresponding mean. Intraclass correlation coefficients (ICCs) were also used to evaluate test-retest variability. Intraclass correlation coefficients greater than 0.75 were considered to indicate good reproducibility.

The statistical analyses were performed with commercially available software (Stata, version 12; StataCorp). The alpha level (type I error) was set at .05.

Results

The investigation of the ability of the nGoggle to detect visual field loss included 62 eyes of 33 patients with glaucoma and 30 eyes of 17 healthy participants. **Table 1** summarizes the clinical and demographic variables for the study participants. There was no statistically significant difference in mean (SD) age between participants with glaucoma and healthy participants (68.2 [11.0] vs 66.1 [9.9]; $P = .57$). There were also no statistically significant differences in race/ethnicity or sex between participants with glaucoma and healthy participants.

The mean (SD) nGoggle global mfSSVEP parameter was lower for eyes with glaucoma (0.289 [0.02]) compared with healthy eyes (0.334 [0.02]; $P < .001$) (Table 1). **Table 2** shows AUCs and sensitivities at fixed specificities for the different nGoggle and SAP parameters. The AUC for the global nGoggle mfSSVEP parameter was 0.92 (95% CI, 0.86-0.96), which was larger than that for SAP MD (AUC, 0.81; 95% CI, 0.72-0.90; $P = .046$), SAP mean sensitivity (AUC, 0.80; 95% CI, 0.69-0.88; $P = .03$), and SAP PSD (AUC, 0.77; 95% CI, 0.66-0.89; $P = .01$). **Figure 2** shows ROC curves for the mfSSVEP-CCA parameter and for MD. For specificity at 80%, the mfSSVEP CCA parameter had sensitivity of 85% compared with 64% for SAP MD. For specificity at 90%, the mfSSVEP-CCA parameter had sensitivity of 71% vs 43% for SAP MD.

Figure 2. Receiver Operating Characteristic Curves for the Global nGoggle Parameter and Standard Automated Perimetry Mean Deviation

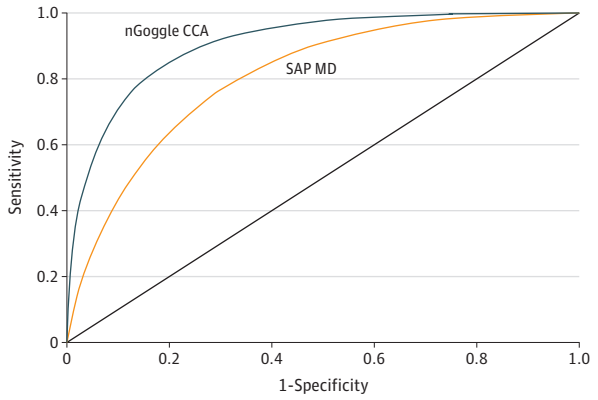

Receiver operating characteristic curves for the nGoggle global multifocal steady state visual-evoked potential parameter and standard automated perimetry mean deviation (SAP MD).

The eTable in the Supplement shows ROC curve areas for sectoral measurements obtained by the nGoggle and SAP. The ROC curve areas were generally larger for nGoggle than for SAP, notably for the central area, although there was not a statistically significant difference between the corresponding sectors ($P > .10$ for all comparisons).

Figure 3 illustrates an example of test results obtained by the nGoggle in a glaucomatous and a healthy eye, as well as SAP results in the same eyes.

Assessment of Repeatability

The repeatability of measurements obtained by the nGoggle was investigated in 20 eyes of 10 participants with glaucoma. These eyes had a median SAP MD of −3.7 dB, ranging from −21.7 dB to 0.1 dB. The mean global mfSSVEP value on all tests results was 0.289, ranging from 0.248 to 0.347. The average ICC of the global mfSSVEP parameter was 0.92 (95% CI, 0.82-0.97), which was greater than 0.75 ($P < .001$). The ICCs for sectors ranged from 0.74 to 0.90. The mean coefficient of variation of the mfSSVEP global parameter was 3.03% (95% CI, 2.19%-3.87%), whereas the coefficients of variation for sectors ranged from 4.14% to 7.45%.

Discussion

In this study, we described and provided an initial validation of the nGoggle, a portable BCI device for objectively assessing visual field loss. The proposed device integrates an EEG and a head-mounted display for assessing mfSSVEP potentials in response to visual stimulation. Our results showed that the nGoggle was able to discriminate eyes with glaucomatous neuropathy from healthy eyes. Additionally, measurements from the nGoggle showed adequate test-retest repeatability, suggesting that they may be useful for longitudinally monitoring neural losses.

Steady state VEP signals obtained by the nGoggle were significantly lower in glaucomatous compared with healthy eyes, with an AUC of 0.92. The ROC curve area for the global mfSSVEP parameter was superior to those obtained for SAP global parameters mean sensitivity, MD, and PSD. To allow an unbiased comparison between the diagnostic accuracies of SAP and the nGoggle, a glaucoma diagnosis was based on the masked assessment of optic disc photographs. This approach has been used by several authors when investigating and comparing the diagnostic accuracies of multiple visual function tests for glaucoma. Sample et al[36] reported ROC curve areas ranging from 0.60 to 0.80 for different SAP parameters when detecting glaucoma diagnosed based on the assessment of optic disc photographs. Importantly, damage to the optic disc and retinal nerve fiber layer as seen on photographs has been shown to precede and predict the development of visual field defects in many eyes with glaucoma.[37-39] In our study, 11 (18%) of the 62 eyes with glaucomatous optic neuropathy had SAP MD and PSD with $P > 5\%$, as well as Glaucoma Hemifield Test (GHT) results within normal limits, as compared with the Humphrey normative database, and would be classified as having normal fields in clinical practice. These eyes had an average (SD) global mfSSVEP of 0.280 (0.010), which was significantly lower than that of the healthy eyes included in the study (0.334 [0.024]; $P < .001$). This finding suggests that the mfSSVEP signals obtained by the nGoggle may be able to detect glaucoma before the appearance of visual field defects on standard perimetry, a finding that has been previously shown in studies with conventional (nonsteady state) and wet-electrode–based multifocal VEP devices in glaucoma.[2,40-42]

Although ROC curve areas tended to be larger for sectoral measurements from the nGoggle compared with SAP, no statistically significant differences were noted. Notably, the largest difference was seen for the central sector, with ROC curve areas of 0.81 vs 0.68, respectively. This might reflect the relative insensitivity of the SAP 24-2 strategy for detecting glaucomatous damage in the central area.[43]

Assessing the repeatability of the nGoggle showed that its measurements exhibited low test-retest variability. The ICC was 0.92 and the coefficient of variation was 3.03% for the global mfSSVEP-CCA parameter. These numbers are comparable with those previously described for traditional wired and wet-electrode multifocal VEP assessment.[44] The low test-retest variability of the nGoggle seems to reflect the stability of SSVEP potentials and their known relatively high SNR and less susceptibility to artifacts, supporting its application for assessing longitudinal change over time. However, future longitudinal studies are necessary to investigate the ability of the device to detect progressive glaucomatous damage over time.

Limitations

Our study was intended to perform an initial proof-of-concept of the feasibility of the nGoggle as a portable objective device for assessment of visual function. The portability and objectivity make the device promising for a home-based assessment of visual function. With home-based testing, a much higher number of test results could be acquired, potentially making it easier to separate true change from test-retest variability.

Figure 3. Results From the nGoggle and Standard Perimetry of Glaucomatous and Healthy Eyes

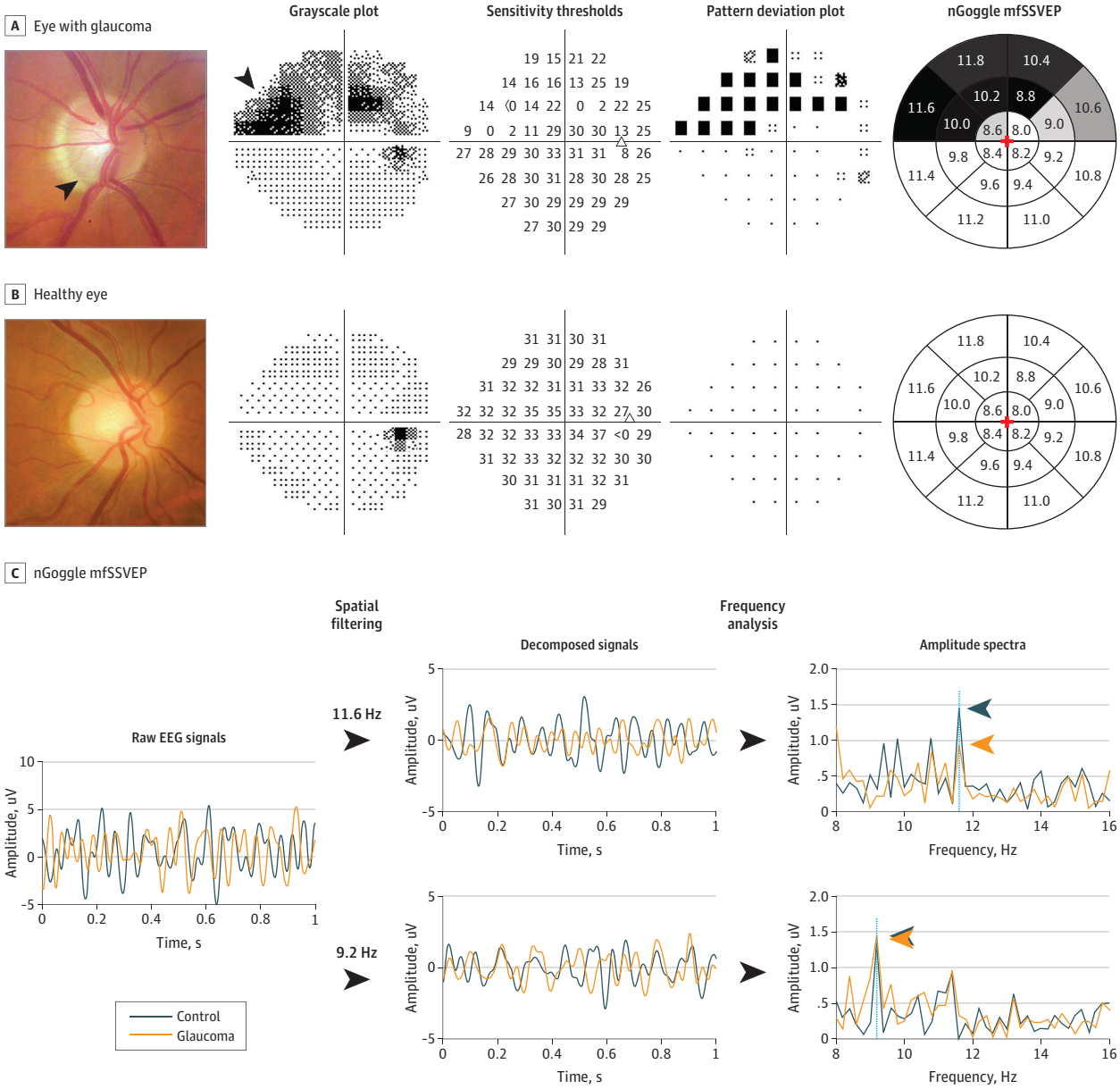

A. Eye with glaucoma showing inferior loss of neuroretinal rim (arrowhead) and superior nasal visual field defect (arrowhead). B. Optic disc photograph and perimetric results of a healthy eye. C. Multifocal steady state visual evoked potentials (mfSSVEP) obtained by the nGoggle for the eyes in A (orange) and B (blue). The figure illustrates processing for sectors 11.6Hz, located in the superior nasal region of defect; and 9.2Hz, located in the inferior temporal normal region. For the 11.6Hz frequency, the amplitude for the glaucoma eye (orange arrowhead) is much lower than that for the healthy eye (blue arrowhead). For the 9.2Hz frequency, the amplitudes are almost identical. The final pattern of nGoggle sectoral results are show in greyscale in the rightmost column. EEG indicates electroencephalogram.

Although our study only investigated using the nGoggle in a controlled office-based setting, in a previous study, we have shown the feasibility of acquiring reliable wireless SSVEP signals among participants performing ordinary activities, such as walking on a treadmill.[45] It is important to recognize, however, that home-based testing is likely to introduce unforeseen challenges and, therefore, carefully conducted studies will be necessary to validate the device for this application.

Conclusions

We presented the development and application of a BCI device as a portable platform for objectively assessing visual function. The device was able to identify eyes with glaucomatous optic neuropathy and its measurements showed adequate repeatability. Future longitudinal investigations should assess whether BCI devices are able to detect progressive glaucomatous damage.

ARTICLE INFORMATION

Accepted for Publication: March 4, 2017.

Published Online: April 27, 2017. doi:10.1001/jamaophthalmol.2017.0738

Author Contributions: Dr Medeiros had full access to all the data in the study and takes responsibility for the integrity of the data and the accuracy of the data analysis. Drs Nakanishi and Y.-T. Wang contributed equally to this work.
Concept and design: Nakanishi, Y.-T. Wang, Jung, Daga, Medeiros.
Acquisition, analysis, or interpretation of data: All authors.
Drafting of the manuscript: Nakanishi, Y.-T. Wang, Jung, Daga, Medeiros.
Critical revision of the manuscript for important intellectual content: All authors.
Statistical analysis: Y.-T. Wang, Jung, Daga, Medeiros.
Obtained funding: Jung, Medeiros.
Administrative, technical, or material support: Jung, Zao, Medeiros.
Supervision: Jung, Medeiros.

Conflict of Interest Disclosures: All authors have completed and submitted the ICMJE Form for Disclosure of Potential Conflicts of Interest. Drs Jung, Zao, and Medeiros report being cofounders of nGoggle, Inc. Dr Medeiros receives research support from Alcon Laboratories, Bausch & Lomb, Carl Zeiss Meditec, Heidelberg Engineering, Merck, Allergan, Sensimed, Topcon, and Reichert and is a consultant for Allergan, Carl Zeiss Meditec, and Novartis. No other disclosures were reported.

Funding/Support: This research was supported by the National Institutes of Health/National Eye Institute grants EY021818 and R21 EY025056, the University of California–San Diego Calit2 Strategic Research Opportunity, and grant CTA W911NF-10-2-0022 from the Army Research Laboratory.

Role of the Funder/Sponsor: The funders had no role in the design and conduct of the study; collection, management, analysis, and interpretation of the data; preparation, review, or approval of the manuscript; and decision to submit the manuscript for publication.

REFERENCES

1. Chauhan BC, Garway-Heath DF, Goñi FJ, et al. Practical recommendations for measuring rates of visual field change in glaucoma. *Br J Ophthalmol*. 2008;92(4):569-573.

2. Hood DC, Thienprasiddhi P, Greenstein VC, et al. Detecting early to mild glaucomatous damage: a comparison of the multifocal VEP and automated perimetry. *Invest Ophthalmol Vis Sci*. 2004;45(2):492-498.

3. Vialatte FB, Maurice M, Dauwels J, Cichocki A. Steady-state visually evoked potentials: focus on essential paradigms and future perspectives. *Prog Neurobiol*. 2010;90(4):418-438.

4. Perlstein WM, Cole MA, Larson M, Kelly K, Seignourel P, Keil A. Steady-state visual evoked potentials reveal frontally-mediated working memory activity in humans. *Neurosci Lett*. 2003;342(3):191-195.

5. Gray M, Kemp AH, Silberstein RB, Nathan PJ. Cortical neurophysiology of anticipatory anxiety: an investigation utilizing steady state probe topography (SSPT). *Neuroimage*. 2003;20(2):975-986.

6. Abdullah SN, Aldahlawi N, Rosli Y, Vaegan, Boon MY, Maddess T. Effect of contrast, stimulus density, and viewing distance on multifocal steady-state visual evoked potentials (MSVs). *Invest Ophthalmol Vis Sci*. 2012;53(9):5527-5535.

7. Abdullah SN, Vaegan, Boon MY, Maddess T. Contrast-response functions of the multifocal steady-state VEP (MSV). *Clin Neurophysiol*. 2012;123(9):1865-1871.

8. Vaegan, Rahman AM, Sanderson GF. Glaucoma affects steady state VEP contrast thresholds before psychophysics. *Optom Vis Sci*. 2008;85(7):547-558.

9. Vaegan, Anderton PJ, Millar TJ. Transient and steady state focal and pattern electroretinogram nerve section losses in cats with unilateral optic. *Doc Ophthalmol*. 2002;105(2):105-127.

10. Wang Y, Wang R, Gao X, Hong B, Gao S. A practical VEP-based brain-computer interface. *IEEE Trans Neural Syst Rehabil Eng*. 2006;14(2):234-239.

11. Bin G, Gao X, Yan Z, Hong B, Gao S. An online multi-channel SSVEP-based brain-computer interface using a canonical correlation analysis method. *J Neural Eng*. 2009;6(4):046002.

12. Chi YM, Jung TP, Cauwenberghs G. Dry-contact and noncontact biopotential electrodes: methodological review. *IEEE Rev Biomed Eng*. 2010;3:106-119.

13. Zhang Z, Jung TP, Makeig S, Rao BD. Compressed sensing for energy-efficient wireless telemonitoring of noninvasive fetal ECG via block sparse Bayesian learning. *IEEE Trans Biomed Eng*. 2013;60(2):300-309.

14. Zhang Z, Jung TP, Makeig S, Rao BD. Compressed sensing of EEG for wireless telemonitoring with low energy consumption and inexpensive hardware. *IEEE Trans Biomed Eng*. 2013;60(1):221-224.

15. Lin CT, Ko LW, Chang MH, et al. Review of wireless and wearable electroencephalogram systems and brain-computer interfaces--a mini-review. *Gerontology*. 2010;56(1):112-119.

16. Mullen T, Kothe C, Chi YM, et al. Real-time modeling and 3D visualization of source dynamics and connectivity using wearable EEG. *Conf Proc IEEE Eng Med Biol Soc*. 2013;2013:2184-2187.

17. Gramann K, Gwin JT, Ferris DP, et al. Cognition in action: imaging brain/body dynamics in mobile humans. *Rev Neurosci*. 2011;22(6):593-608.

18. Gramann K, Gwin JT, Bigdely-Shamlo N, Ferris DP, Makeig S. Visual evoked responses during standing and walking. *Front Hum Neurosci*. 2010;4:202.

19. Gwin JT, Gramann K, Makeig S, Ferris DP. Removal of movement artifact from high-density EEG recorded during walking and running. *J Neurophysiol*. 2010;103(6):3526-3534.

20. Delorme A, Sejnowski T, Makeig S. Enhanced detection of artifacts in EEG data using higher-order statistics and independent component analysis. *Neuroimage*. 2007;34(4):1443-1449.

21. Onton J, Westerfield M, Townsend J, Makeig S. Imaging human EEG dynamics using independent component analysis. *Neurosci Biobehav Rev*. 2006;30(6):808-822.

22. Delorme A, Makeig S. EEGLAB: an open source toolbox for analysis of single-trial EEG dynamics including independent component analysis. *J Neurosci Methods*. 2004;134(1):9-21.

23. Makeig S, Westerfield M, Jung TP, et al. Dynamic brain sources of visual evoked responses. *Science*. 2002;295(5555):690-694.

24. Jung TP, Makeig S, McKeown MJ, Bell AJ, Lee TW, Sejnowski TJ. Imaging brain dynamics using independent component analysis. *Proc IEEE Inst Electr Electron Eng*. 2001;89(7):1107-1122.

25. Jung TP, Makeig S, Westerfield M, Townsend J, Courchesne E, Sejnowski TJ. Removal of eye activity artifacts from visual event-related potentials in normal and clinical subjects. *Clin Neurophysiol*. 2000;111(10):1745-1758.

26. Jung TP, Makeig S, Humphries C, et al. Removing electroencephalographic artifacts by blind source separation. *Psychophysiology*. 2000;37(2):163-178.

27. Nakanishi M, Wang Y, Wang YT, Mitsukura Y, Jung TP. A high-speed brain speller using steady-state visual evoked potentials. *Int J Neural Syst*. 2014;24(6):1450019.

28. Nakanishi M, Wang Y, Wang YT, Jung TP. A comparison study of canonical correlation analysis based methods for detecting steady-state visual evoked potentials. *PLoS One*. 2015;10(10):e0140703.

29. Chen X, Wang Y, Nakanishi M, Gao X, Jung TP, Gao S. High-speed spelling with a noninvasive brain-computer interface. *Proc Natl Acad Sci U S A*. 2015;112(44):E6058-E6067.

30. Nakanishi M, Wang Y, Wang YT, Mitsukura Y, Jung TP. Generating visual flickers for eliciting robust steady-state visual evoked potentials at flexible frequencies using monitor refresh rate. *PLoS One*. 2014;9(6):e99235.

31. Wang Y, Wang YT, Jung TP. Visual stimulus design for high-rate SSVEP BCI. *Electron Lett*. 2010;46(15):1057-1058. doi:10.1049/el.2010.0923

32. Wang Y, Gao X, Gao S. Computational modeling and application of steady-state visual evoked potentials in brain-computer interfaces. *Sci Suppl*. 2015;350(6256):43-46. https://www.researchgate.net/profile/Yijun_Wang5/publication/282679100_Computational_modeling_and_application_of_SSVEPs_in_BCIs/links/5618704f08ae6d17308498ea.pdf.

33. Lin Z, Zhang C, Wu W, Gao X. Frequency recognition based on canonical correlation analysis for SSVEP-based BCIs. *IEEE Trans Biomed Eng*. 2007;54(6 Pt 2):1172-1176.

34. Garway-Heath DF, Poinoosawmy D, Fitzke FW, Hitchings RA. Mapping the visual field to the optic disc in normal tension glaucoma eyes. *Ophthalmology*. 2000;107(10):1809-1815.

35. Medeiros FA, Sample PA, Zangwill LM, Liebmann JM, Girkin CA, Weinreb RN. A statistical approach to the evaluation of covariate effects on the receiver operating characteristic curves of diagnostic tests in glaucoma. *Invest Ophthalmol Vis Sci*. 2006;47(6):2520-2527.

36. Sample PA, Medeiros FA, Racette L, et al. Identifying glaucomatous vision loss with

visual-function-specific perimetry in the diagnostic innovations in glaucoma study. *Invest Ophthalmol Vis Sci*. 2006;47(8):3381-3389.

37. Gordon MO, Beiser JA, Brandt JD, et al. The Ocular Hypertension Treatment Study: baseline factors that predict the onset of primary open-angle glaucoma. *Arch Ophthalmol*. 2002;120(6):714-720.

38. Medeiros FA, Alencar LM, Zangwill LM, Bowd C, Sample PA, Weinreb RN. Prediction of functional loss in glaucoma from progressive optic disc damage. *Arch Ophthalmol*. 2009;127(10):1250-1256.

39. Quigley HA, Katz J, Derick RJ, Gilbert D, Sommer A. An evaluation of optic disc and nerve fiber layer examinations in monitoring progression of early glaucoma damage. *Ophthalmology*. 1992;99(1):19-28.

40. Hood DC, Greenstein VC. Multifocal VEP and ganglion cell damage: applications and limitations for the study of glaucoma. *Prog Retin Eye Res*. 2003;22(2):201-251.

41. Goldberg I, Graham SL, Klistorner AI. Multifocal objective perimetry in the detection of glaucomatous field loss. *Am J Ophthalmol*. 2002;133(1):29-39.

42. Graham SL, Klistorner AI, Goldberg I. Clinical application of objective perimetry using multifocal visual evoked potentials in glaucoma practice. *Arch Ophthalmol*. 2005;123(6):729-739.

43. Hood DC, Raza AS, de Moraes CG, Liebmann JM, Ritch R. Glaucomatous damage of the macula. *Prog Retin Eye Res*. 2013;32:1-21.

44. Punjabi OS, Stamper RL, Bostrom AG, Lin SC. Repeatability of the multifocal visual evoked potentials in a clinical glaucoma setting. *Can J Ophthalmol*. 2008;43(4):435-440.

45. Lin YP, Wang Y, Jung TP. Assessing the feasibility of online SSVEP decoding in human walking using a consumer EEG headset. *J Neuroeng Rehabil*. 2014;11:119.